Supported by

Characteristics of ELM precursors on NSTX

P. Ridha
with contribution from:
J.E. Menard, K. Tritz, D. Stutman,
R. Maingi, E. Fredrickson and H. Zohm

Annual APS Meeting
of the Division of Plasma Physics
Monday, October 24, 2005
Denver, Colorado

ASDEX Upgrade

PPPL PRINCETON PLASMA PHYSICS LABORATORY

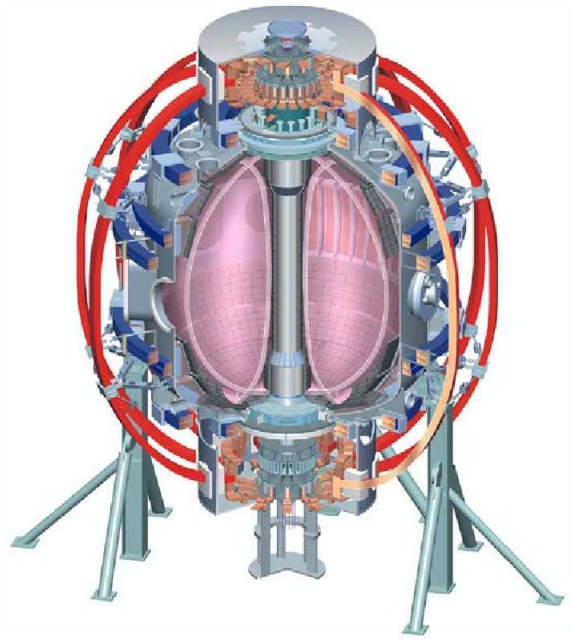

Abstract

The precursor characteristics of Edge Localized Modes (ELMs) on NSTX were analyzed with Mirnov and USXR diagnostics in terms of toroidal mode number, growth rate, precursor oscillation periods and frequcency, and edge localization. Mode identification is especially difficult for most ELMs studied, as the precursor growth rates are often comparable to the oscillation period. Details of the mode identification process will be described. The Mirnov diagnostic does not tell whether the ELM is edge localized or not, thus the USXR array was used to discriminate between the edge and core plasma using an analysis of the X-ray emission with different metallic filters (Ti $0.4\mu m$ - $E_{cut-off}100eV$, Be $10\mu m$ - $E_{cut-off}500eV$, Be $100\mu m$ - $E_{cut-off}1.2keV$). Using the titanium filter, a strong correlation between Mirnov and USXR data during an ELM crash was observed. Analysis of the USXR data using a constrained tomographic inversion shows relative USXR fluctuation amplitudes from ELM precursors in the range of 1% to 5%. This analysis combined with an edge displacement model provides an estimate of the transient boundary displacements for typical ELMs of $\lesssim 5$ mm.

Outline

- Mirnov and USXR ELM Precursor Diagnostic
- Energy Sensitivity with Different Filters Separates Edge and Core Radiation
- Toroidal Mode Number Identification Process
- Discrimination of Mode's Edge Localization
- ELM Crash Impact on Mirnov and USXR Data
- Analysis of USXR's ELM Crash Signal
- Comparison Type I ELM vs. $\nu_*^{e,ped}$ (ASDEX Upgrade vs. NSTX)
- Summary and Results

Mirnov and USXR
ELM Precursor Diagnostic

Magnetic confined fusion plasma is not constant in time and space, so the growing ELMs are evolving in time, are moving periodically (in a helical way) around the torus.
The following simulation[1] shows the calculated flow velocity v and the electron temperature T_e (poloidal cross section) at the plasma edge during an ELM activity.

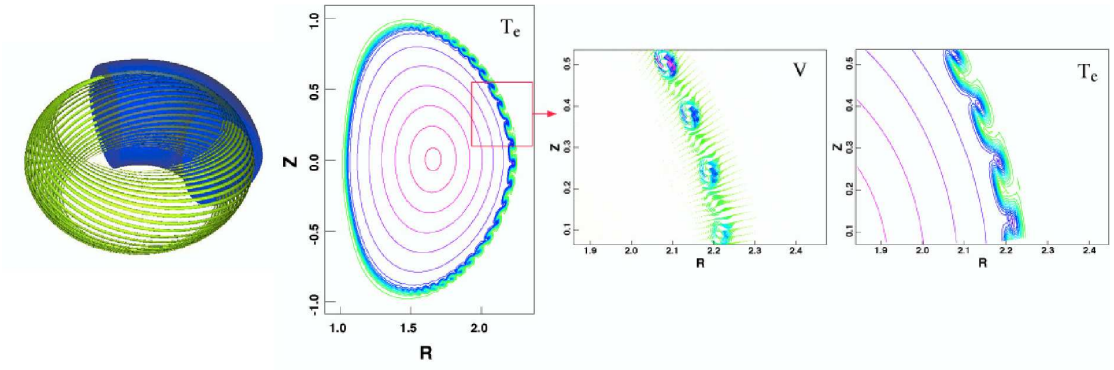

Thus, ELMs can be observed by stroboscopic detection technique in order to study the ELM crash pre-history by

1. fast diagnostic technique (e.g. Mirnov coils for dB/dt signal),
2. fast fourier transformation (FFT) (i.e. stroboscopic observation),
3. toroidal and poloidal mode number ELM characterization.

[1]BRENNAN D.P. (MIT, Cambridge,MA). *Nonlinear Simulations of ELMs with NIMROD*. APS - Talk 2004.

Mirnov and USXR
ELM Precursor Diagnostic

The ELM crash relevant signals are illustrated here:

- Ultrasoft X-ray signals measured with two different[2] cameras
- CIII spectral line and D_α signal
- Integrated and frequency filtered[3] Mirnov signal B(t)

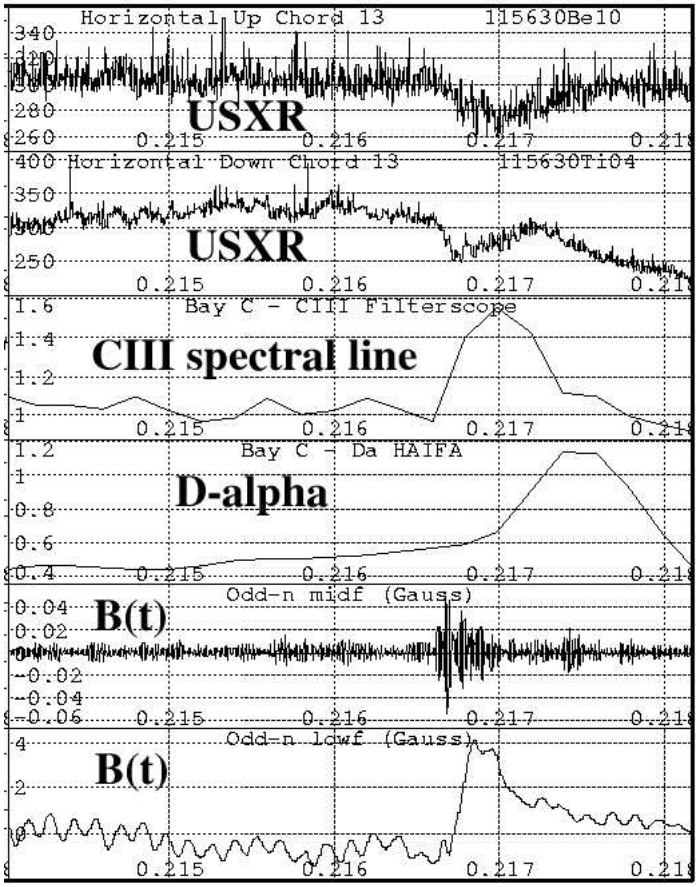

⇒ During an ELM crash the (integrated) mid frequency filtered Mirnov signal B(t) shows the characteristics of a typical ELM precursor.

[2]Horizontal Up and Horizontal Down USXR cameras at chord number 13.
[3]Low and mid frequency Hanning filters have been applied.

Mirnov and USXR
ELM Precursor Diagnostic

USXR diagnostic characteristics:

- 10 eV... 500 eV energy emission
- Capability to analyze plasma core and periphery[4]
- Four pinhole cameras (silicion diodes) with fast time response (few μs) and high time resolution
- Line of sight integrated X-ray intensity ($dI = \varepsilon dl$)

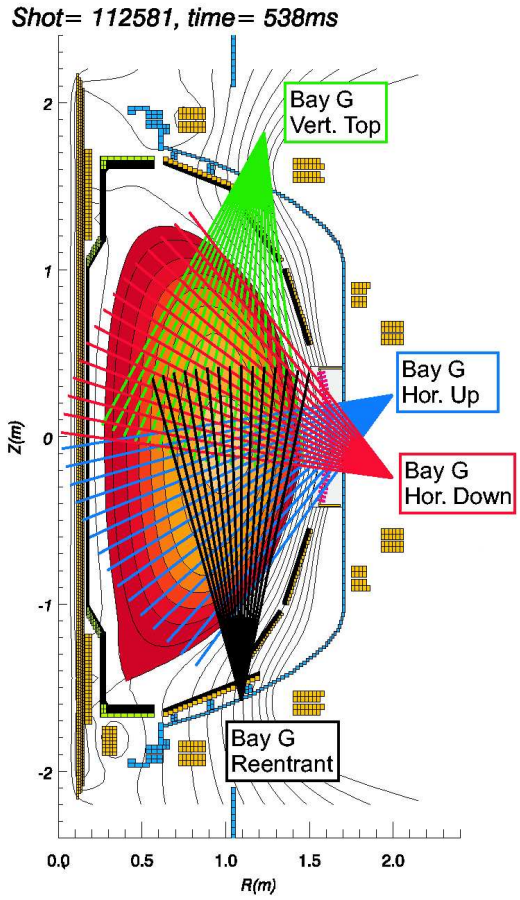

[4]STUTMAN D. et al. *Ultrasoft x-ray imaging system for the National Spherical Torus Experiment.* Rev. Sci. Instrum. **68**, 572 (1999).

Energy Sensitivity with Different Filters Separates Edge and Core Radiation

USXR emission analyzed with three different metallic filters:

- Ti $0.4\mu m$ - $E_{cut-off}100eV$,
- Be $10\mu m$ - $E_{cut-off}500eV$ and
- Be $100\mu m$ - $E_{cut-off}1.2keV$

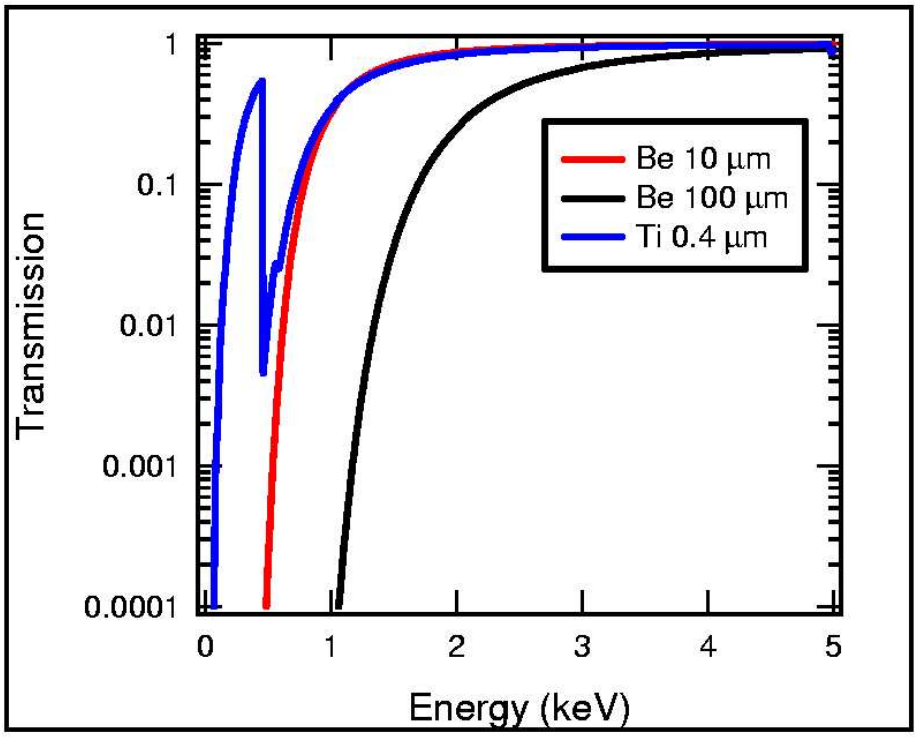

The titanium filter emphasizes more the plasma edge, while with the two beryllium filters it is possible to observe the plasma core.

Toroidal Mode Number Identification Process

- Algorithm tries to reconstruct previously integrated and filtered B(t) signal by a phase fit of the measured mode phase.
- Assuming a harmonic mode[5] and a constant poloidal mode number m (for constant magnetic flux surface) then the measured B(t) signal can be approximated as $B(n, \hat{B}) \sim \hat{B} \cdot e^{i(n\varphi)}$ (with amplitude $\hat{B}$), while $\varphi = \varphi_{sensor}$ is fixed and the toroidal mode # n will be varied.
- Transferring latter into a matrix algorithm like

$$A_{ni} \cdot x_n = b_i \Leftrightarrow \begin{bmatrix} A_{00} & \dots & A_{n0} \\ \vdots & \ddots & \vdots \\ A_{0i} & \dots & A_{ni} \end{bmatrix} \cdot \begin{bmatrix} x_0 \\ \vdots \\ x_n \end{bmatrix} = \begin{bmatrix} b_0 \\ \vdots \\ b_i \end{bmatrix}$$

  where $A_{ni} = e^{i\psi_i}$ is the harmonic mode term (corresponds to $\hat{B}$), $x_n = \rho e^{i\tau}$ is the complex amplitude for the toroidal mode number n (with fit amplitude ρ and arbitrary phase of fit τ) and $b_i = \beta_i e^{i\Phi_i}$ is the complex magnetic measurement at toroidal angle Φ_i.
- Assuming $\psi_i = -in\Phi_i$ (with measurement index i) for a given trial toroidal mode number n then the phase fit algorithm solves

$$\rho e^{i(\Phi_i + \tau)} = \beta_i e^{i\Phi_i}$$

  where left-hand side is the phase fit value B_{pf} of the magnetic raw data and right-hand side represents the measured magnetic signal. Latter provides the calculated '2π mode phase', which corresponds to the toroidal mode # once plotted vs. Mirnov sensor position.

[5]The measured magnetic field B(t) is approximated through a sum of harmonic modes,

Toroidal Mode Number Identification Process

1. FFT analysis of dB/dt & numerical integration ⇒ B(t)
2. Plot magnetical spectral amplitude vs. frequency (top)
3. Calculate phase fit of B(t) signal ⇒ $B_{pf} = \rho e^{i(\Phi_i + \tau)}$
4. Plot both, B(t) and B_{pf} vs. time (middle)
5. Plot 2π mode phase vs. sensor pos. ⇒ red-square points (bottom)
6. Fit former ⇒ 'sawtooth' line indicates the toroidal mode #

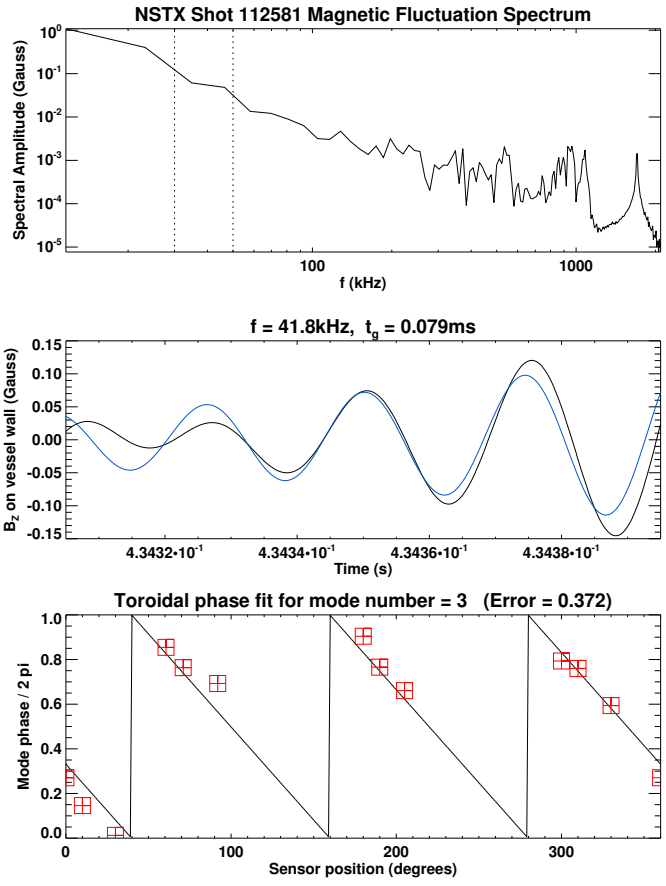

Toroidal Mode Number Identification Process

Best toroidal mode number fit based on following criteria:

- phase fitting error[6] < 0.4
- growthrate $\gamma > 0$ and
- reasonable toroidal mode number n

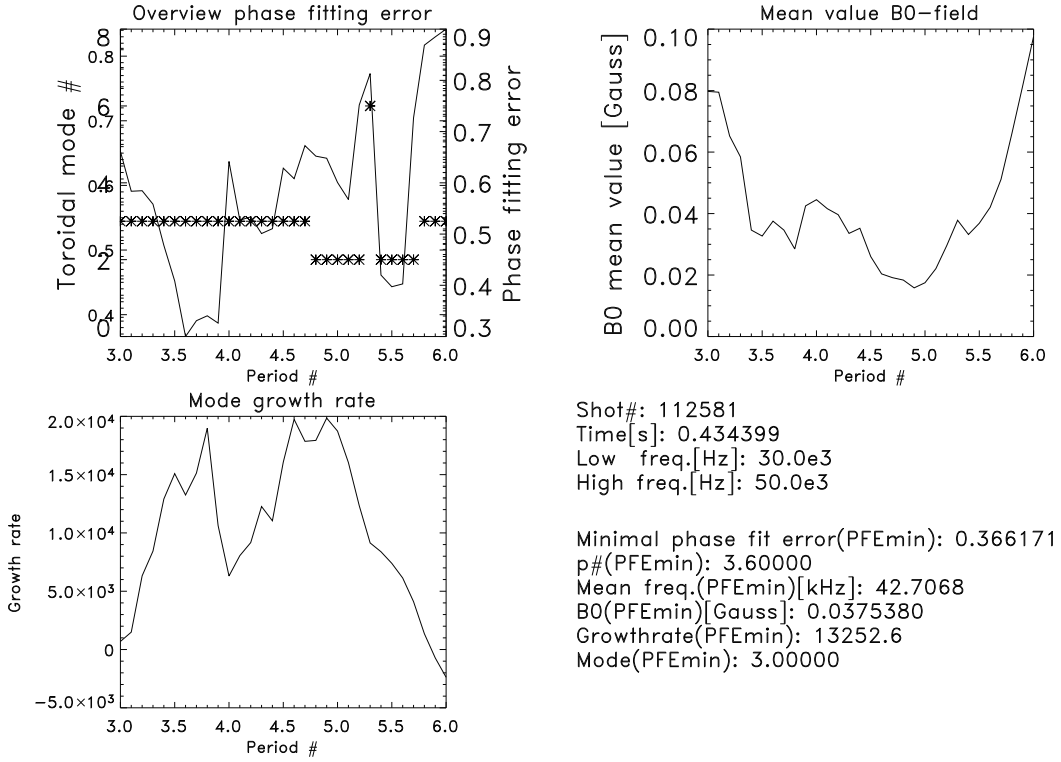

Applying above's criteria and extending the phase fit algorithm with a period number[7] scan, then it is possible to obtain the best toroidal mode number fit for every ELM crash.

[6]The phase fit error is defined as the % difference between B_{pf} and B(t).

[7]That period number corresponds to the period # of precursor oscillations before an ELM crash.

Toroidal Mode Number Identification Process

Overview of the analyzed toroidal mode number fit data during an ELM crash and its precursor oscillations:

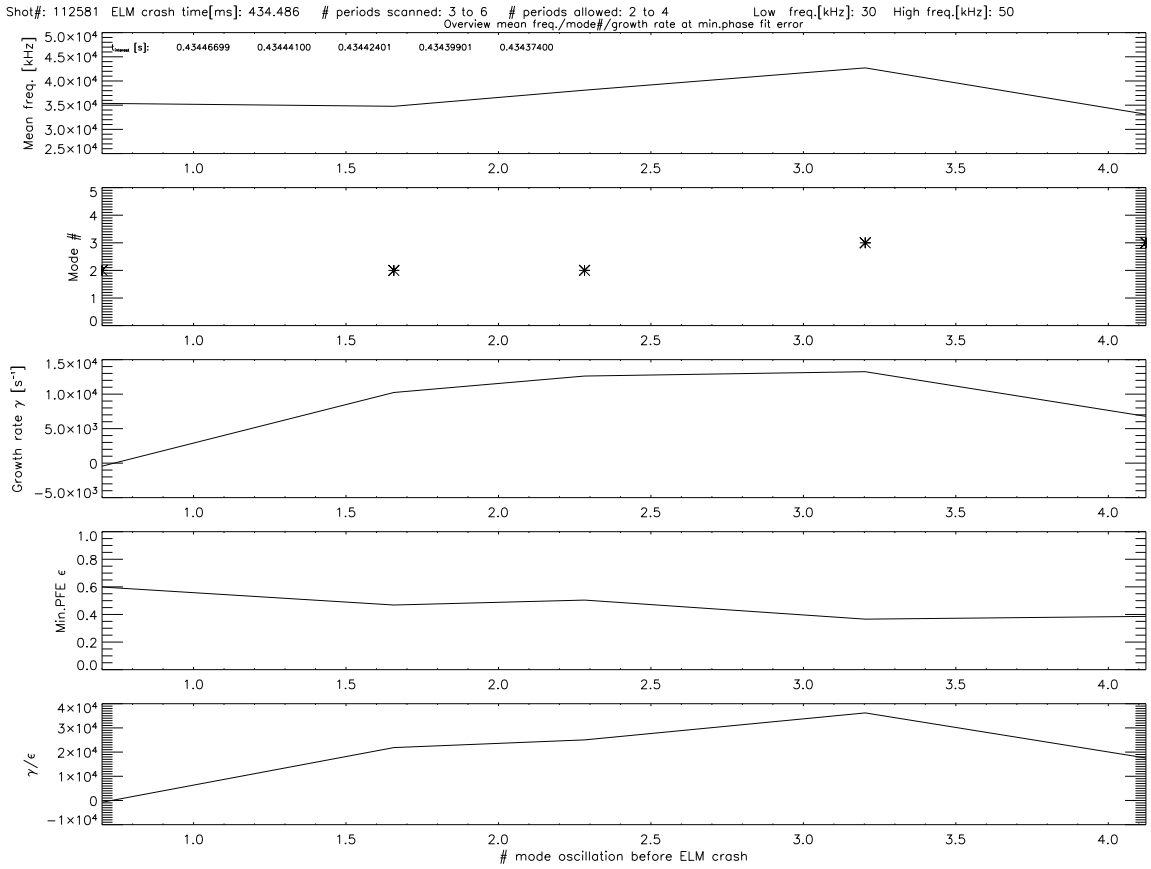

⇒ We observe the ELM precursor propagation frequency to decrease during the mode growth, suggesting the mode may be affecting the toroidal rotation profile.

Discrimination of Mode's Edge Localization

Two dimensional tomographic reconstruction[8] of the measured and filtered (Ti 0.4μm) USXR emissivity shows a so-called 'halo' profile (edge carbon emission), which indicates the edge localization of the mode.

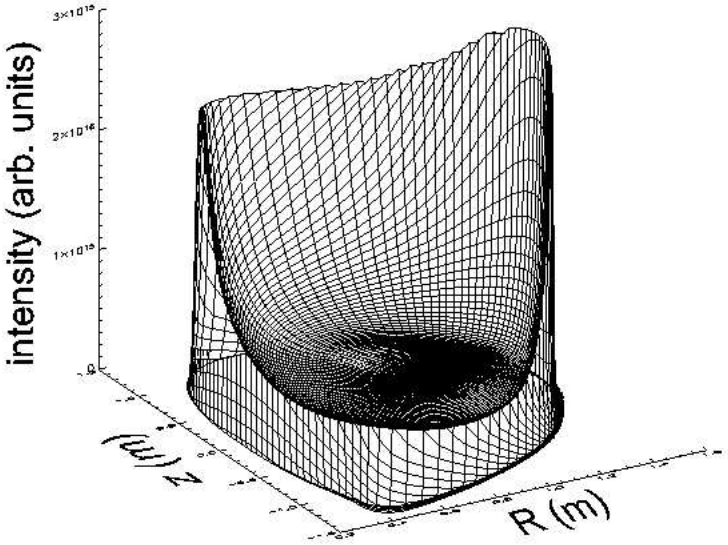

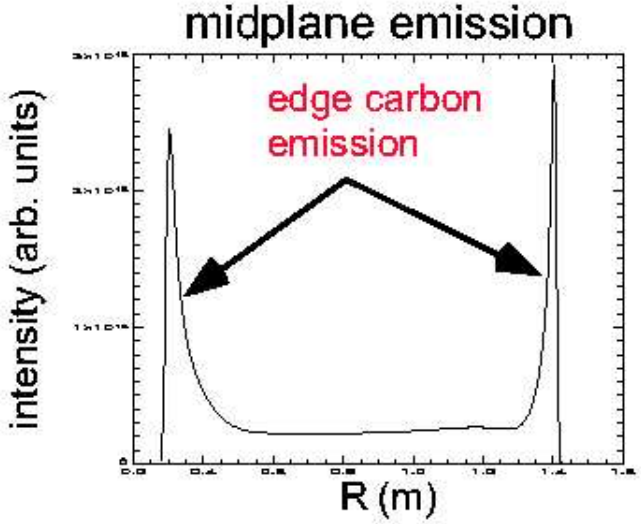

[8]TRITZ K. et al. *Characterization of ELMs and their Effects on NSTX using Multi-color Ultrasoft X-ray Imaging*. APS talk 2004.

ELM Crash Impact on Mirnov and USXR Data

Using the titanium filter Ti $0.4\mu m$ and a band pass frequency filter (30 kHz to 50 kHz) a strong correlation between Mirnov and USXR data during an ELM crash was observed, but ...

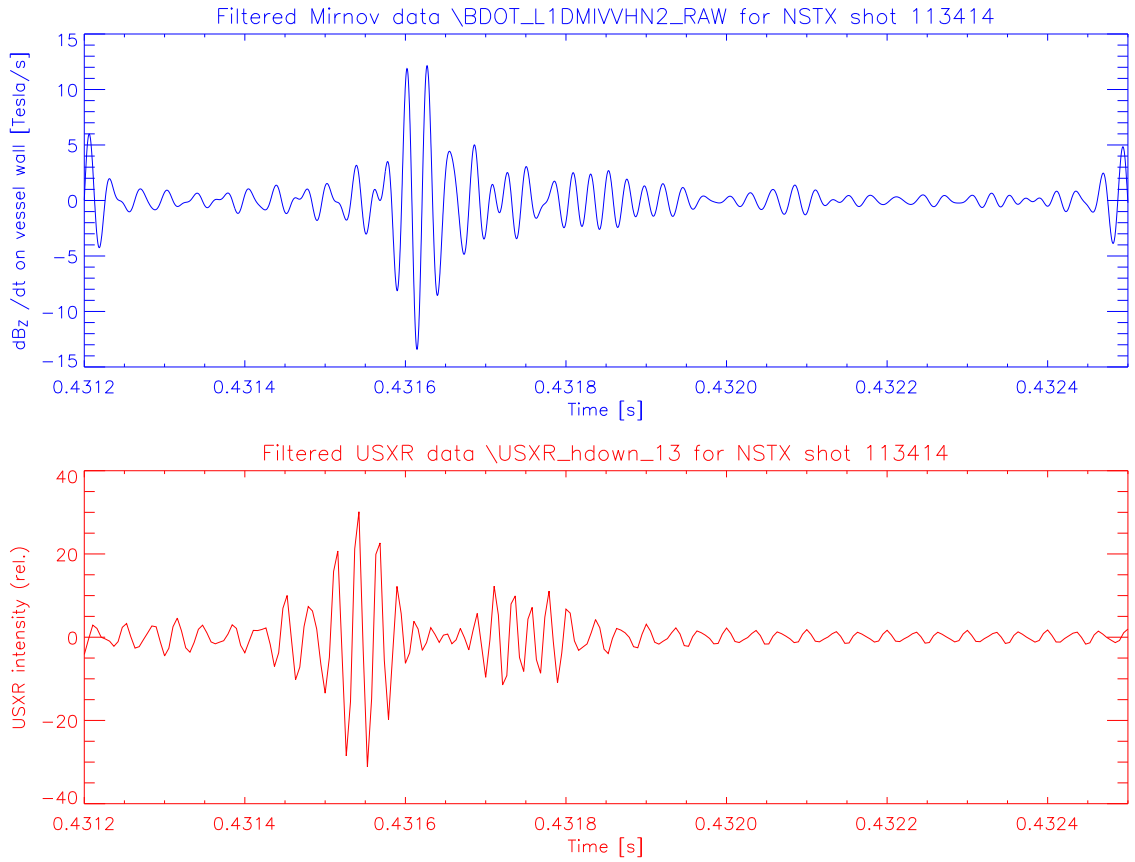

... it is not clear if the phase difference is due to synchronization problems with the data acquisition, or if the precursor is truly perturbing the near-edge equilibrium flux surfaces prior to generating a measurable magnetic perturbation.

Analysis of USXR's ELM Crash Signal

- Correlation between the Mirnov and the Ultrasoft X-ray signal during an ELM applying the emissivity change $\delta\varepsilon \sim \nabla\varepsilon \cdot \boldsymbol{\xi}_\perp$ can be defined as the *relative USXR fluctuation amplitude*[9]

$$\Delta\hat{a} = \frac{\int dl \nabla\varepsilon}{\int dl\varepsilon} \cdot \boldsymbol{\xi}_\perp$$

- From experimental data analysis of the normalized USXR data for several ELM crashes a relative USXR fluctuation amplitude range of $1\% \ldots 5\%$ has been recognized

- Latter demonstrates clearly a correlation between the Mirnov and the USXR signal regarding the detection of ELMs.
  This relative fluctuation amplitude of $1\% \ldots 5\%$, combined with estimates of the radial decay length of perturbed magnetic field, implies a boundary displacement of a few millimeters during precursor growth (see next slide for details).

[9] With the orthogonal displacement vector $\boldsymbol{\xi}_\perp$, the *total USXR emissivity gradient* $\int dl \nabla\varepsilon$ and the *total USXR intensity* $\int dl\varepsilon$.

Analysis of USXR's ELM Crash Signal

In the first two windows the total USXR intensity and the total emissvity gradient are both plotted versus the midplane radius. Here one has to note, that both signals are obtained experimentally, whereas in the third window the assumption of the eigenfunction's radial profile is plotted.

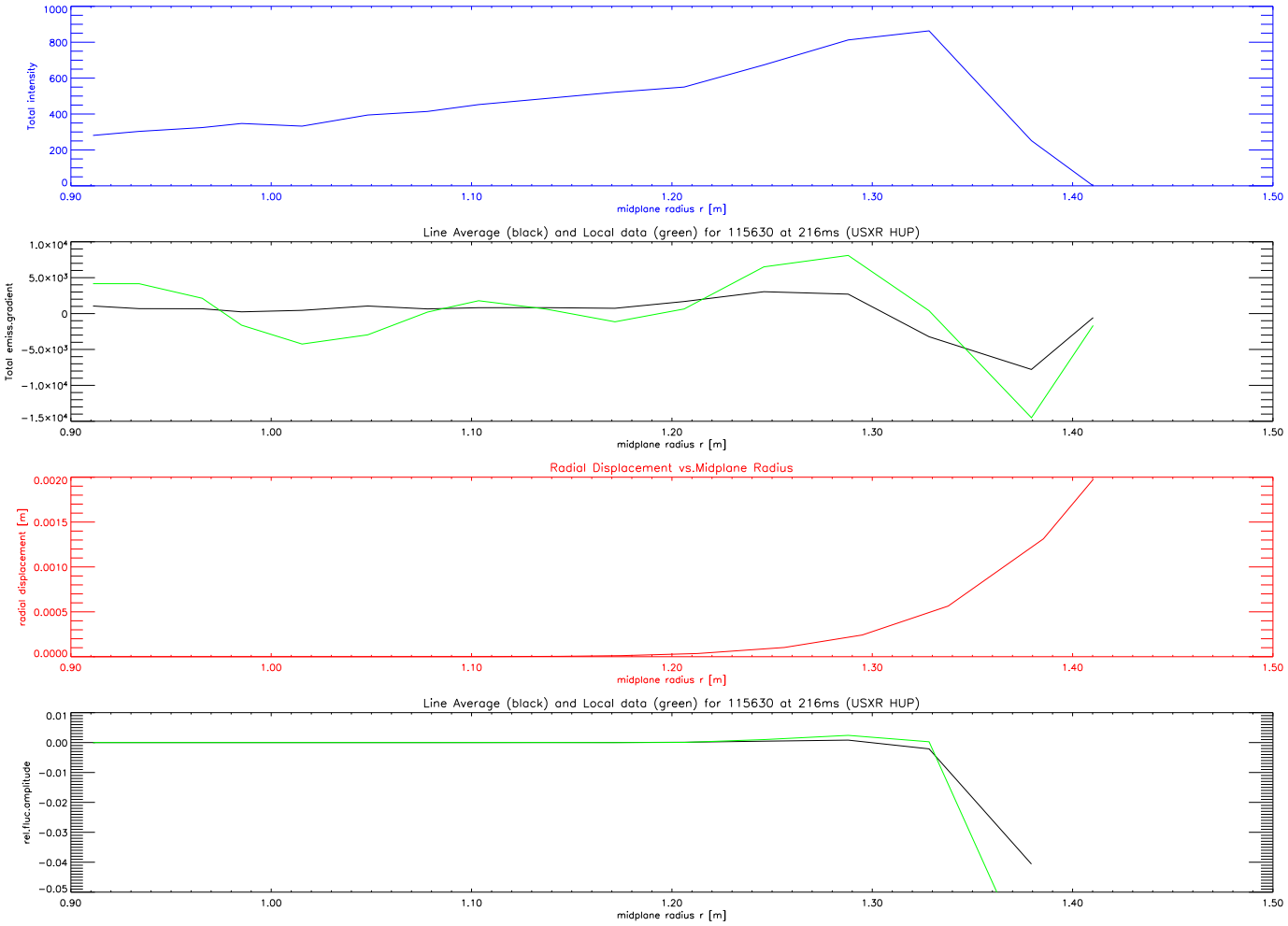

Finally, the fourth window shows the plot combining total intensity, emissivity gradient and assumed eigenfunction's radial profile based on above's equation in order to point out the MHD mode's edge localization observed with the USXR data.

Comparison Type I ELM vs. $\nu_*^{e,ped}$ (ASDEX Upgrade vs. NSTX)

- Electron pedestal top collisionality $\nu_*^{e,ped}(=\nu_*^e)$ was calculated with the formular of *Sauter et al.*[10]

$$\nu_*^{e,ped} = 6.921 \cdot 10^{-18} \frac{q_{95} \cdot R \cdot n_e \cdot Z \cdot \ln \Lambda_e}{T_e^2 \cdot \epsilon^{3/2}}$$

  where ϵ is the inverse aspect ratio a/R and the *electron's Coulomb logarithm* is defined as $\ln \Lambda_e = 31.3 - \ln\left(\sqrt{n_e}/T_e\right)$.

- According to *Maingi et al.*[11] in NSTX large type I ELMs were observed between type V ELMs when $\beta_N \geq 5$, which also corresponds to $\nu_*^{e,ped} \leq 1$ (with $\ln \Lambda_e \approx 15$).

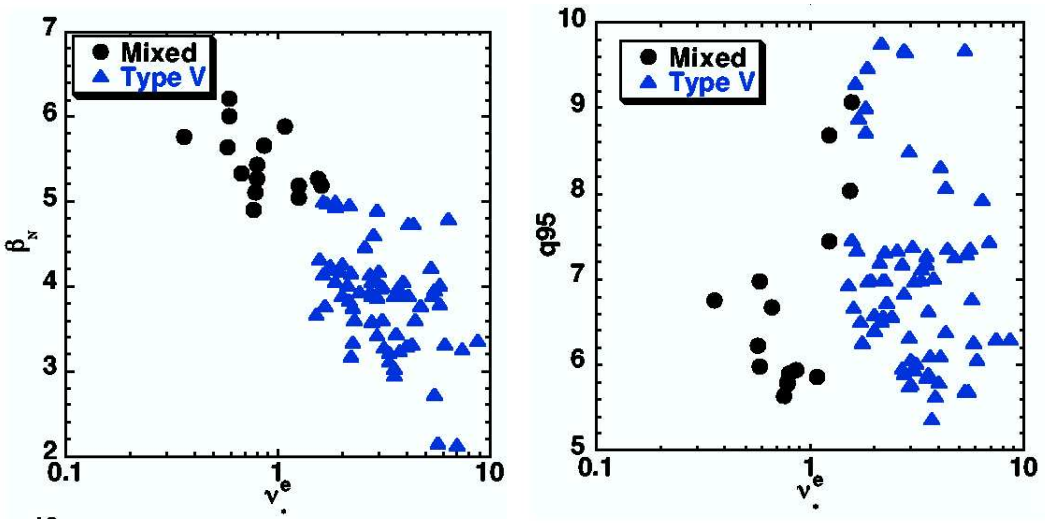

Existence space of type V and mixed type I/V ELMs in β_N vs. ν_*^e (left) and q_{95} vs. ν_*^e (right).

[10] SAUTER O. et al. *Neoclassical conductivity and bootstrap current formulas for general axisymetric equilibria and arbitrary collisionality regime.* Physics of Plasma. Vol.**6**, No.7, p.2834-2839 July 1999.

[11] MAINGI R. et al. *H-mode pedestal, ELM and power threshold studies in NSTX.* Nucl. Fusion **45**, p.1-12 (2005).

Comparison Type I ELM vs. $\nu_*^{e,ped}$ (ASDEX Upgrade vs. NSTX)

The following diagram[12] illustrates the electron density and temperature at the shoulder of the H-mode pedestal at ASDEX Upgrade.

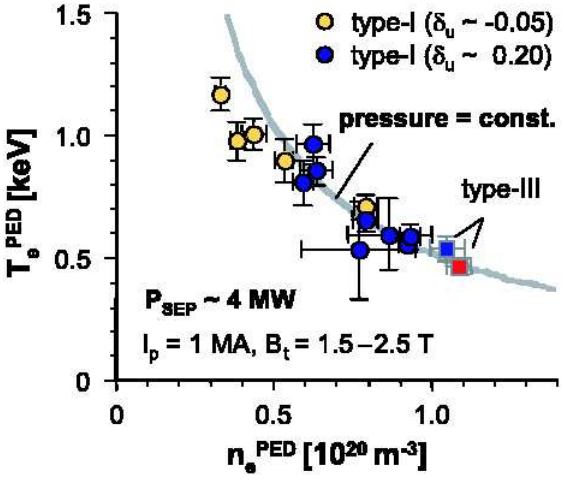

- Applying Sauter's electron pedestal collisionality equation three different $\nu_*^{e,ped}$ values of ASDEX Upgrade's type I ELM along the constant pedestal pressure (grey line) have been calculated.
- In ASDEX Upgrade by a given edge safety factor of $q_{95} = 3.5$, major radius R = 1.7m, Z = 2, $\ln \Lambda_e \approx 17$, ϵ=0.3 the $\nu_*^{e,ped}$ calulations led to the following results:

$$\begin{aligned}
\nu_{*1}^{e,ped}(0.4 \cdot 10^{20} m^{-3}, 1.3keV) &= 0.2016 \\
\nu_{*2}^{e,ped}(1.0 \cdot 10^{20} m^{-3}, 0.5keV) &= 3.4083 \\
\nu_{*3}^{e,ped}(1.3 \cdot 10^{20} m^{-3}, 0.4keV) &= 6.9231
\end{aligned}$$

Note: In above's figure $\nu_{*1}^{e,ped}$ denotes the collisionality far before type III ELMs, while $\nu_{*2}^{e,ped}$ indicates the collisionality close to that ELM kind and $\nu_{*3}^{e,ped}$ is right behind the type III ELM event.

[12] URANO H. et al. *Energy and particle losses during type I ELMy H-mode in ASDEX Upgrade.* Plasma Phys. Controlled Fusion **45**, A1571-1596 (2003).

Comparison Type I ELM vs. $\nu_*^{e,ped}$ (ASDEX Upgrade vs. NSTX)

Due to the fact that the spatial resolution of the edge Thomson scattering measurements at NSTX (left figure) is lower compared to the ASDEX Upgrade one (two figures on the right), only a qualitative comparison of the edge profiles of both fusion experiments was possible.

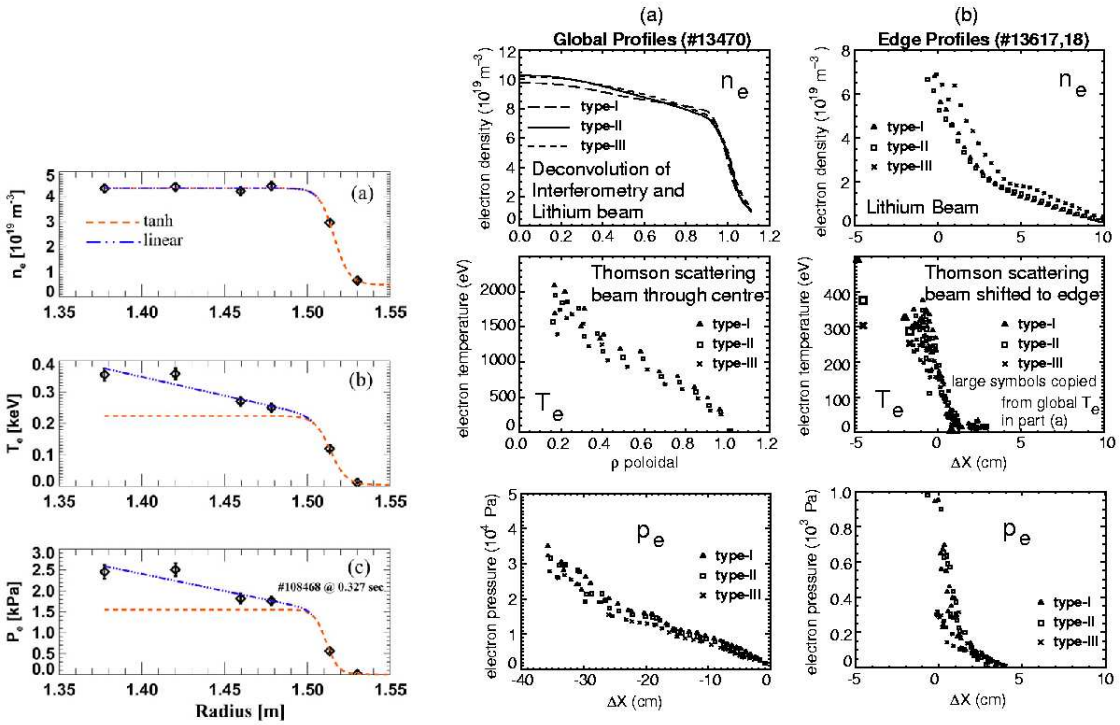

The left figure (taken from *Maingi et al.*) shows typical edge (a) n_e, (b) T_e, (c) P_e profiles and modified hyperbolic tangent fits at NSTX, while the two figures[13] on the right side illustrates the (a) global and the (b) edge profiles for different ELM types at ASDEX Upgrade.

[13]STOBER J. et al. *Type II ELMy H modes on ASDEX Upgrade with good confinement at high density*. Nucl. Fusion **41**, No.9 p.1123-1134 (2001).

Summary and Results

- Toroidal mode number:
  1...4 (for type I ELMs) and 1...5 (for type III ELMs)
- ELM precursor frequencies 30 kHz ... 80 kHz
- ELM precursor oscillation period # 2 ... 4
- clear ELM correlation between Mirnov and USXR data
- type I ELMs on ASDEX Upgrade and NSTX are less prevalent as $\nu_*^e > 1$, perhaps due to a reduced bootstrap current at the plasma edge
- once $\nu_*^{e,ped} \gtrsim 1 \ldots 2$ (at NSTX) then type I ELMs go away
- previous $\nu_*^{e,ped}$ calculations (at ASDEX Upgrade) show similar behaviour and values (within a factor of 2) for both fusion experiments.

Summary and Results

Based on the observation and analyzation of 18 different ELM crashes the following histogram illustrates the statistics of four different ELM types, their toroidal mode numbers n and how many ELMs and related ELM types are happening at a certain toroidal mode number n.

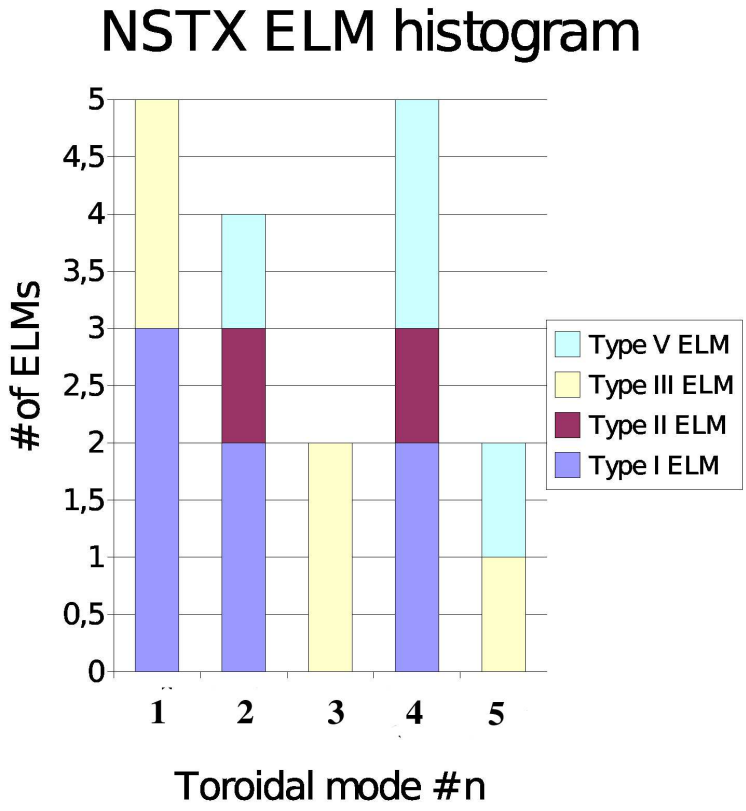

Summary and Results

Statistical ELM analysis:

- In terms of the toroidal mode numbers n = 1 and n = 2 it is obvious that type I ELMs are dominant compared to other ELM types.
- Compared to different ELM types for a toroidal mode number of n = 3 type III ELMs are dominant as well, while type I ELMs and type V ELMs are equal represented for a toroidal mode number of n = 4.
- Also a equal representation is given for type III ELMs and type V ELMs for a toroidal mode number of n = 5.
- Within this statistical analysis for all toroidal mode numbers type II ELMs are least represented.
- Results are preliminary - more ELMs need to be analyzed for NSTX for different ELM types. However, NSTX ELM precursor mode-numbers appear to be a factor of 2 to 3 systematically lower than observed on ASDEX Upgrade, perhaps because of the lower aspect ratio of NSTX.